nature geoscience

SUPPLEMENTARY INFORMATION

https://doi.org/10.1038/s41561-019-0319-5

In the format provided by the authors and unedited.

Role of Asian summer monsoon subsystems in the inter-hemispheric progression of deglaciation

K. Nilsson-Kerr[1*], P. Anand[1*], P. F. Sexton[1], M. J. Leng[2,3], S. Misra[4], S. C. Clemens[5] and S. J. Hammond[1]

[1]School of Environment, Earth and Ecosystem Sciences, Faculty of Science, Technology, Engineering and Mathematics, The Open University, Milton Keynes, UK. [2]NERC Isotope Geoscience Facilities, British Geological Survey, Nottingham, UK. [3]Centre for Environmental Geochemistry, School of Biosciences, University of Nottingham, Loughborough, UK. [4]Centre for Earth Sciences, Indian Institute of Science, Bangalore, India. [5]Earth, Environmental, and Planetary Sciences, Brown University, Providence, RI, USA. *e-mail: katrina.kerr@open.ac.uk; pallavi.anand@open.ac.uk

Role of Asian summer monsoon subsystems in the inter-hemispheric progression of deglaciation

K. Nilsson-Kerr[1*], P. Anand[1], P. F. Sexton[1], M. J. Leng[2], S. Misra[3], S. C. Clemens[4], S. J. Hammond[1]

[1]School of Environment, Earth and Ecosystem Sciences, Faculty of Science, Technology, Engineering and Mathematics, The Open University, Milton Keynes, MK76AA, UK

[2]NERC Isotope Geoscience Facilities, British Geological Survey, Nottingham, NH125GG, UK and Centre for Environmental Geochemistry, School of Biosciences, Sutton Bonington Campus, University of Nottingham, Loughborough, LE12 5RD, UK

[3]Centre for Earth Sciences, Indian Institute of Science, Bangalore, 560012, India

[4]Earth, Environmental, and Planetary Sciences, Brown University, Providence, 02912, USA

([*]katrina.kerr@open.ac.uk)

Supplementary Information

Figures. S1-S12

Tables S1-S2

Supplementary Discussion

Supplementary References

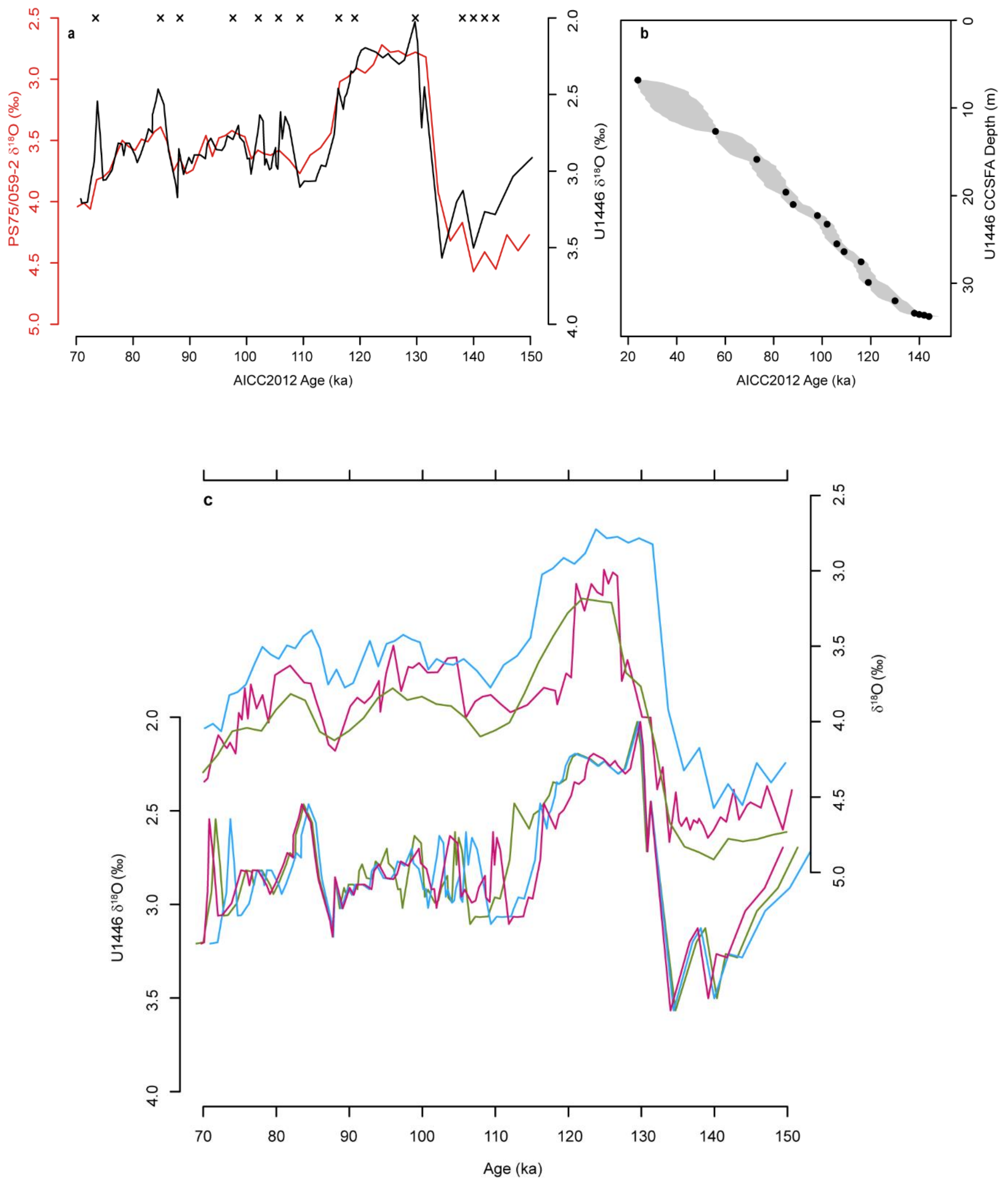

Supplementary Figure 1. U1446 AICC2012 Age Model. Tie points to core PS75/059-2 benthic $\delta^{18}O$ (ref.[61]) indicated by crosses (**a**), Grey shaded area representing 95% confidence interval of the tie points (black filled circles) modelled using Bayesian statistical package Bchron[66] (**b**) and comparison of U1446 benthic $\delta^{18}O$ on AICC2012 (ref.[13]; blue), RC2011 (ref.[63]; pink) and LR04 (ref.[64]; green) chronologies (**c**).

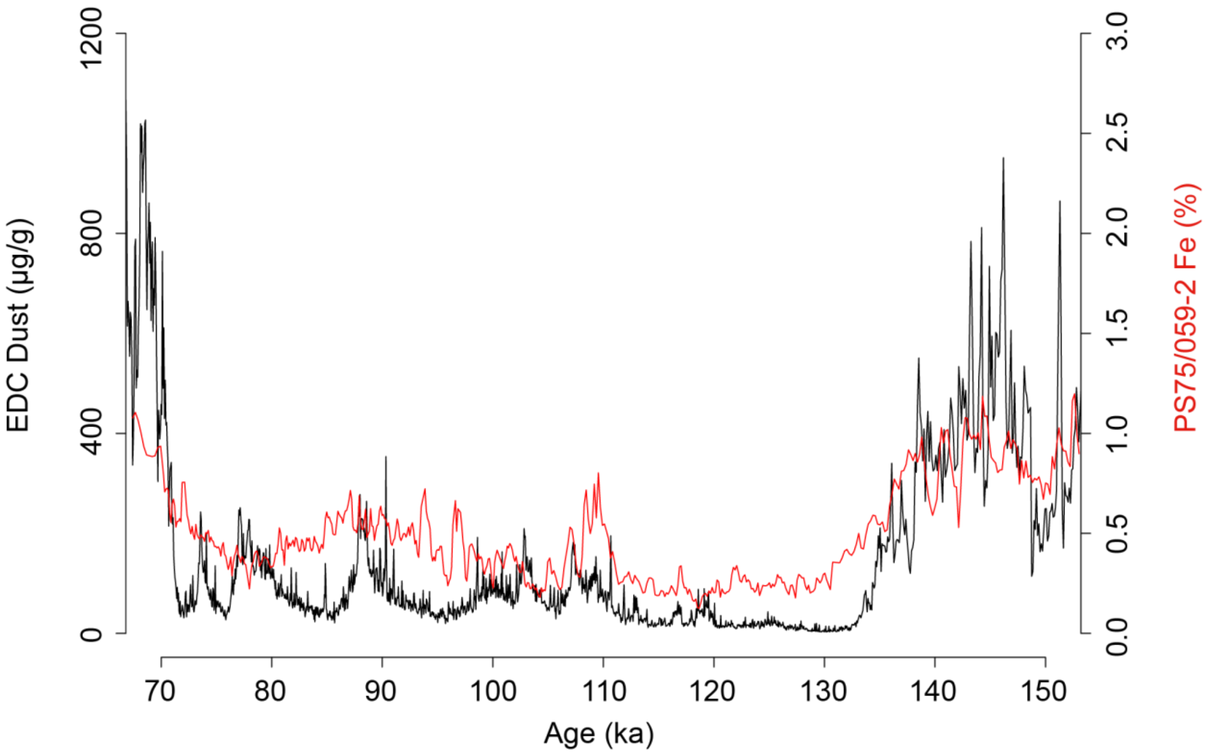

Supplementary Figure 2. Comparison of PS75/059-2 Fe (%) (ref. [62]) with EDC Dust flux[63], both on AICC2012 chronology[13, 62].

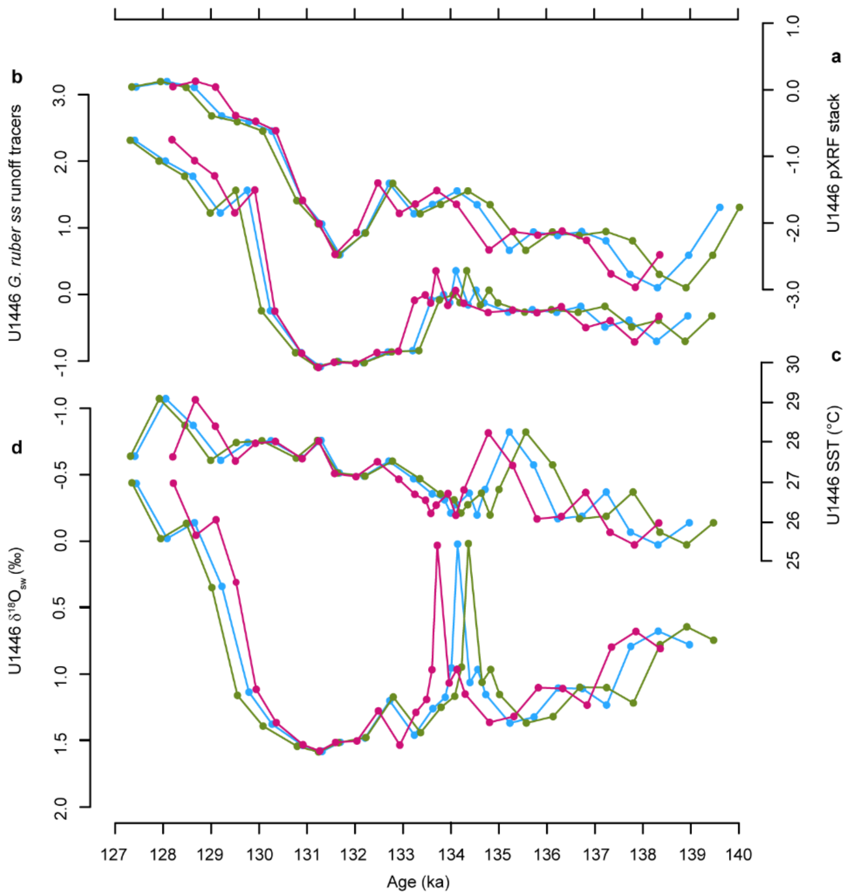

Supplementary Figure 3. Age Model comparison of U1446 ISM proxies. U1446 pXRF stack (**a**), U1446 *G. ruber ss* runoff tracers (**b**), U1446 *G. ruber ss* Mg/Ca derived SST (**c**) and U1446 *G. ruber ss* $\delta^{18}O_{sw}$ on AICC2012 (ref.[13]; blue), RC2011 (ref.[63]; pink) and LR04 (ref.[64]; green) chronologies (**d**).

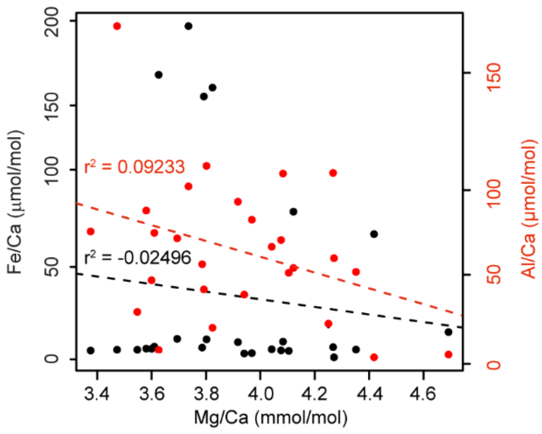

Supplementary Figure 4. *G. ruber ss* Contaminant Indicators. Mg/Ca values plotted against Fe/Ca (black circles) and Al/Ca (red circles) to ensure no bias due to clay contamination in the carbonate bounded foraminifera Mg.

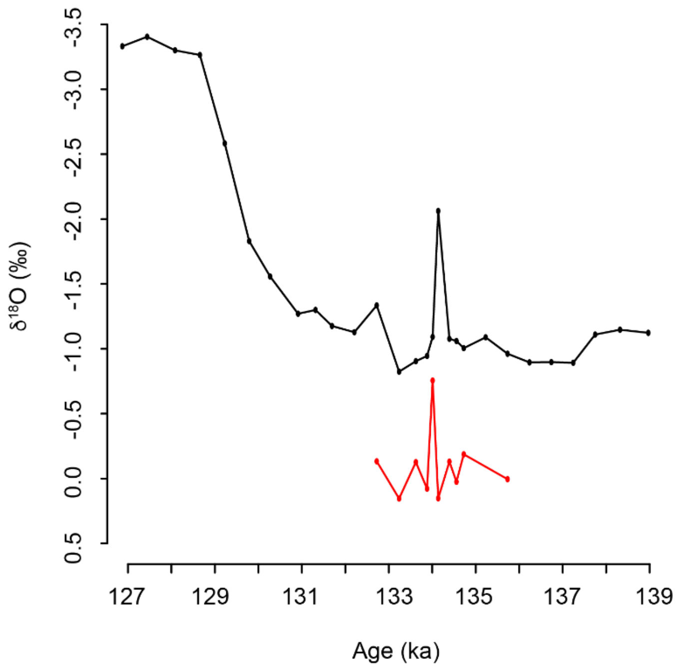

Supplementary Figure 5. Planktic foraminifera δ^{18}O. *G. ruber ss* (black) and *N. dutertrei* (red).

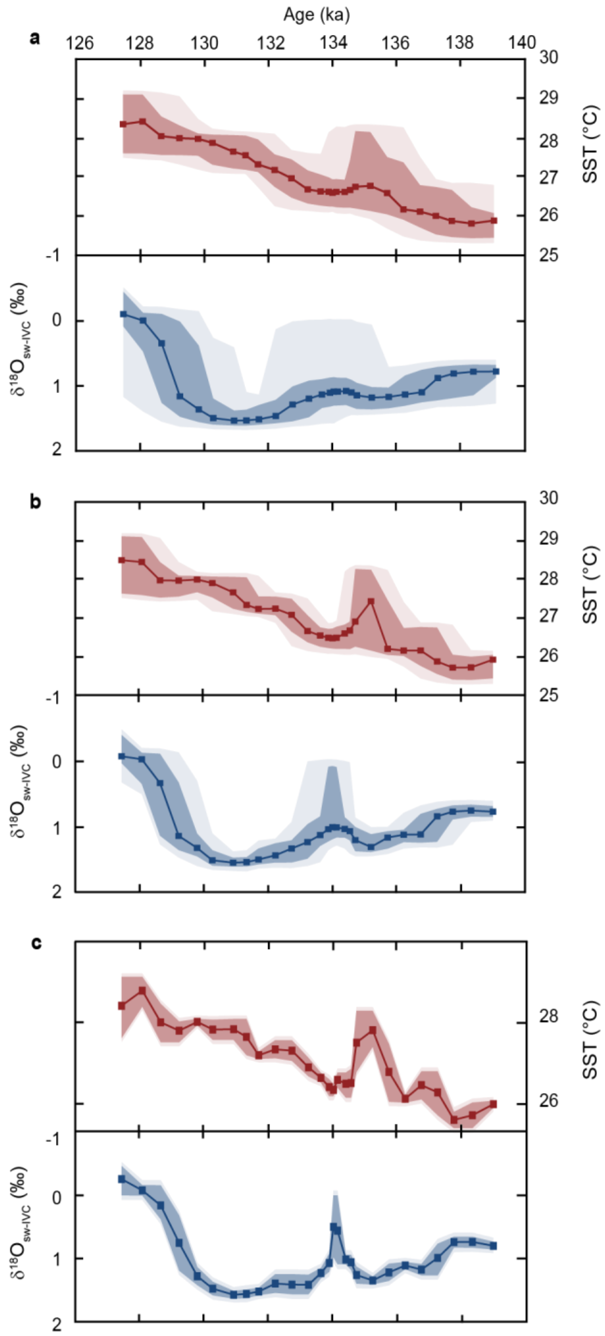

Supplementary Figure 6. PSUSolver[81] Results. SST and $\delta^{18}O_{sw\text{-}IVC}$ confidence intervals (5th, 32nd, 68th and 95th percentiles) - 2 ka age model error (**a**), 1 ka age model error (**b**) and no age model error (**c**).

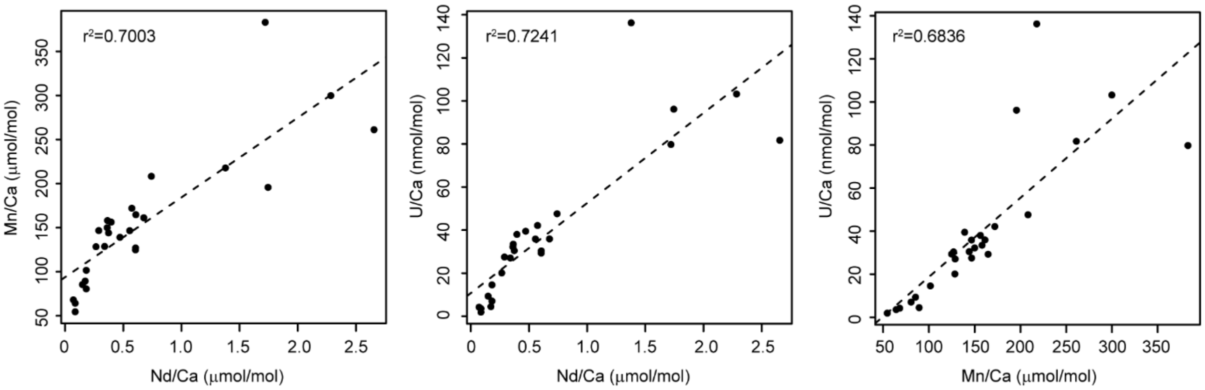

Supplementary Figure 7. Cross-plots of Mn/Ca, Nd/Ca and U/Ca in *G. ruber ss* to identify correlation for deriving a combined runoff tracer.

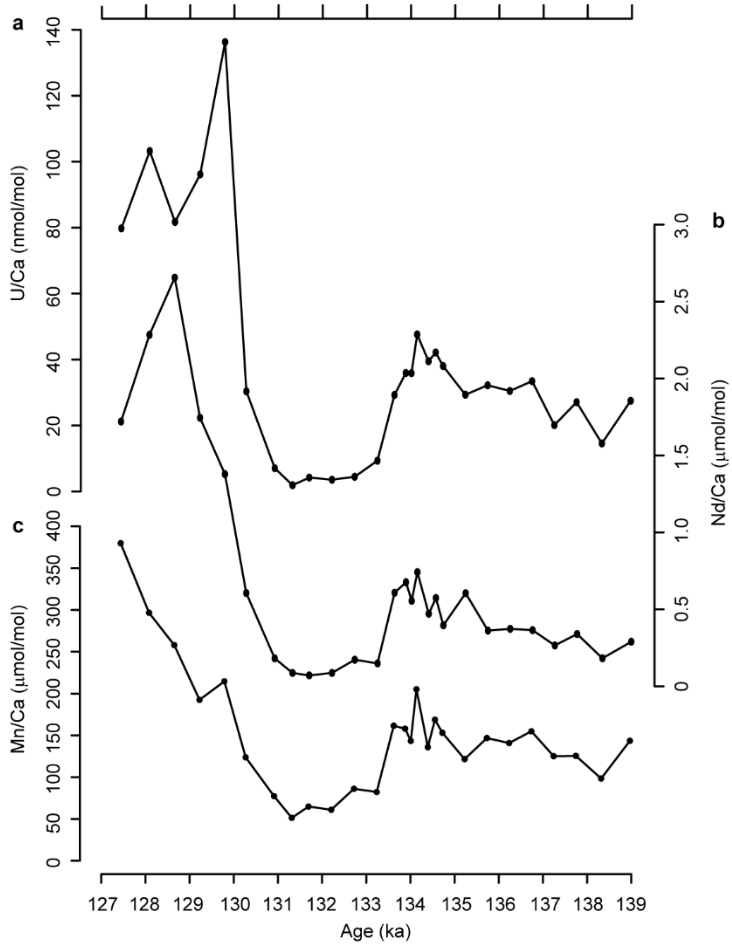

Supplementary Figure 8. Variation in *G. ruber ss*. U/Ca (**a**), Nd/Ca (**b**) and Mn/Ca (**c**) between 139 to 127 ka.

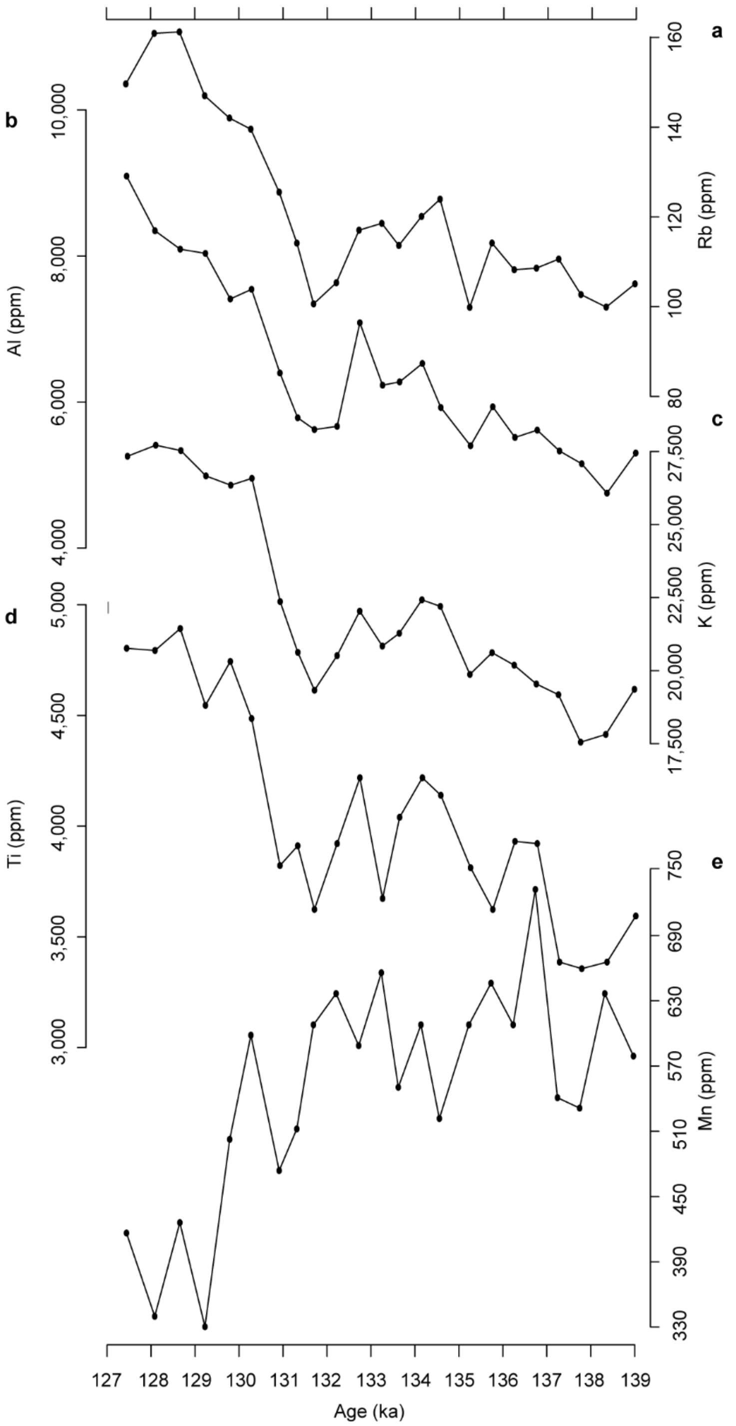

Supplementary Figure 9. pXRF calibrated element concentrations. Rb (**a**), Al (**b**), K (**c**), Ti (**d**) and Mn (**e**) (see information on standards used in calibration in supplementary table 1).

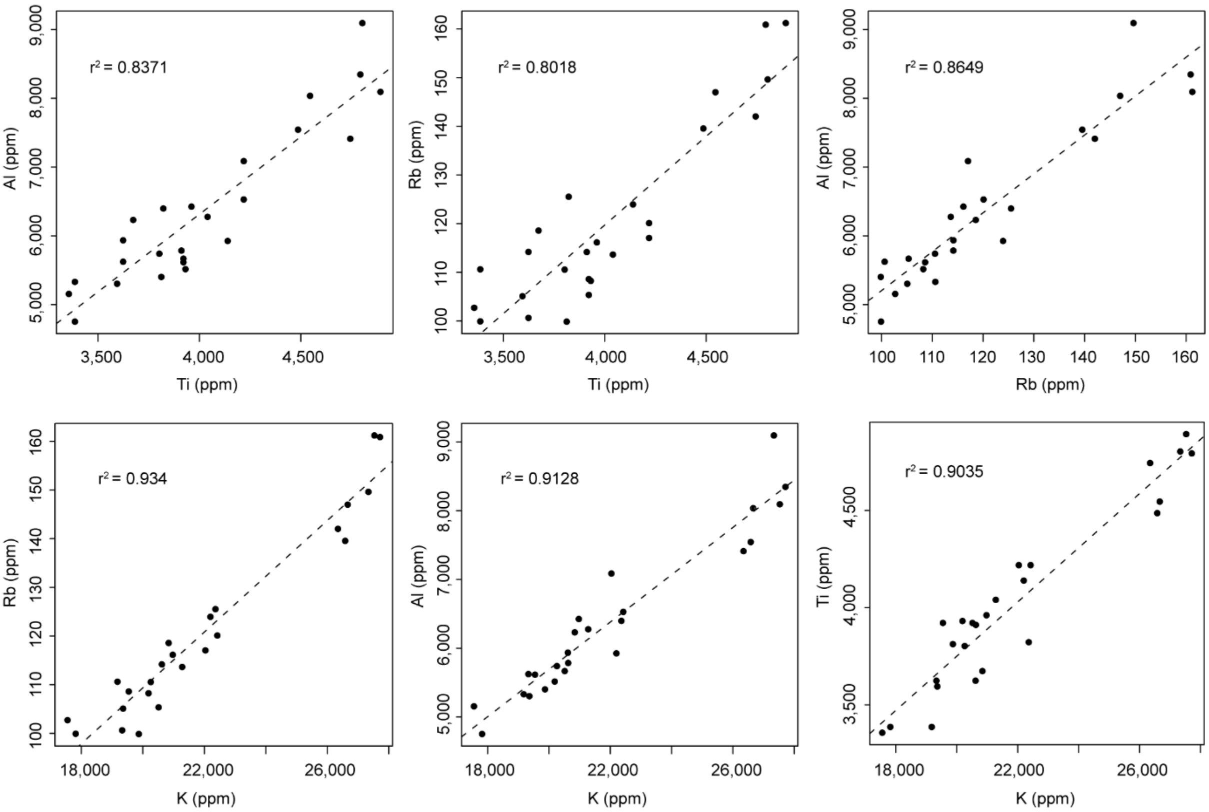

Supplementary Figure 10. Cross-plots showing correlation of terrigenous inferred elements to support pXRF stacking procedure.

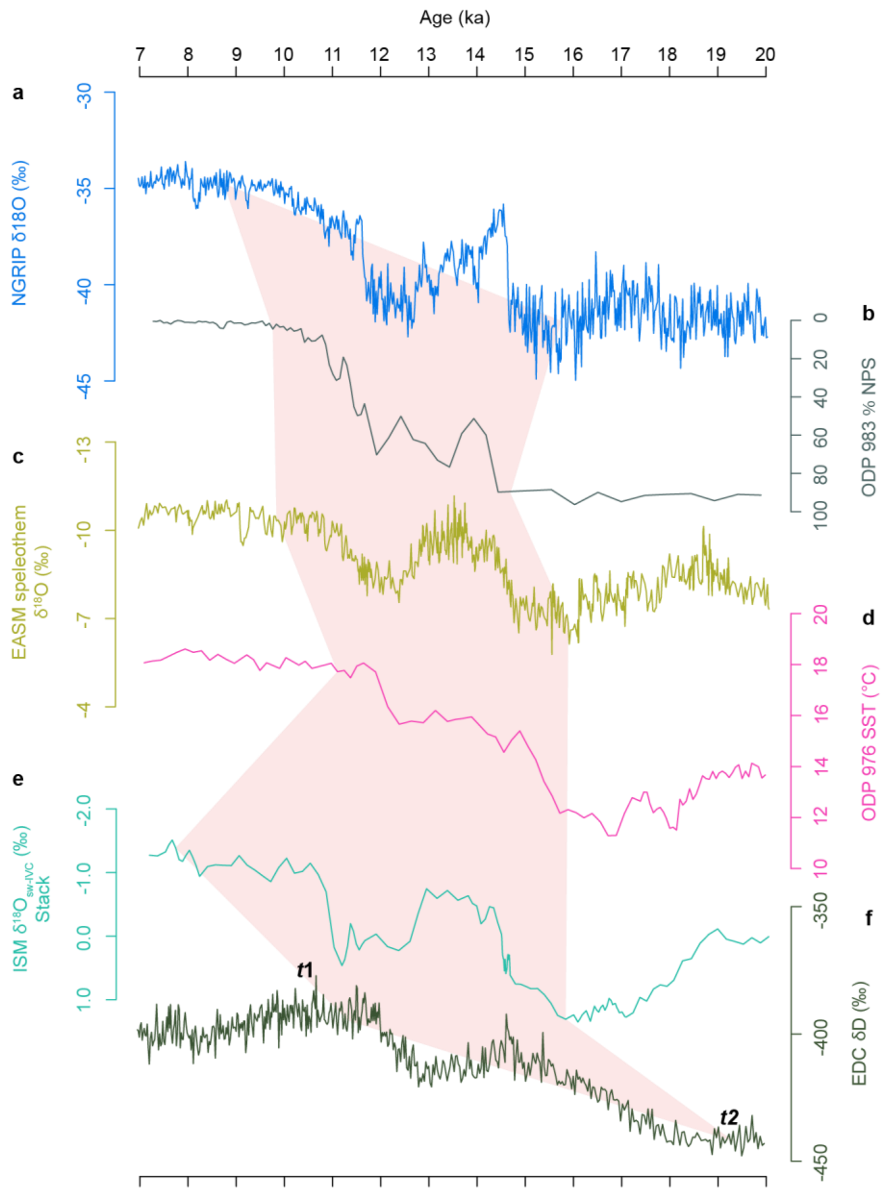

Supplementary Figure 11. Relative timing of TI. NGRIP $\delta^{18}O$ (refs. [96, 97]; **a**), ODP 983 % NPS[48] (**b**), EASM speleothem $\delta^{18}O$ (ref. [6]; **c**), ODP 976, western Mediterranean, SST[29] (**d**), ISM $\delta^{18}O_{sw\text{-}IVC}$ stack[49-51] (**e**) and EDC δD[53] (**f**). Pink shaded area denotes *t*2 (deglaciation onset) and *t*1 (attainment of interglacial) as modelled using RAMPFIT[36].

n	Standard	Ti	K	Al	Rb
44	SDO-1 USGS	0.387	0.246	0.836	0.465
33	MSAN GEOPT15	0.451	0.490	1.307	1.139
9	sDAR-L2 GEOPT37A	1.227	0.200	0.179	0.597
20	U1446 Internal Std. 1	0.417	0.536	0.954	0.577
18	U1446 Internal Std. 2	0.712	0.598	1.230	0.288

Supplementary Table 1. % Relative standard error of reference and internal standards used for pXRF quality control.

	ODP 983 % NPS	ODP 1063 % Warm Species	EASM Speleothem $\delta^{18}O$	ODP 976 SST	EPICA Dome C δD	U1446 pXRF Stack	U1446 *G. ruber ss* runoff tracers	U1446 $\delta^{18}O_{sw}$
*t*1	128.454 ± 0.099	128.453 ± 0.169	128.488 ± 0.025	127.800 ± 0.110	129.418 ± 0.084	128.654 ± 0.388	128.654 ± 0.227	128.654 ± 0.211
*x*1	14.745 ± 2.717	39.529 ± 4.060	-10.372 ± 0.044	20.097 ± 0.110	-372.417 ± 0.596	0.137 ± 0.075	2.039 ± 0.140	-0.223 ± 0.130
*t*2	129.303 ± 0.265	129.161 ± 0.148	129.111 ± 0.032	130.725 ± 0.075	135.553 ± 0.088	131.693 ± 0.429	130.270 ± 0.196	129.788 ± 0.089
*x*2	76.291 ± 1.735	6.438 ± 1.064	-7.445 ± 0.034	13.708 ± 0.096	-437.423 ± 0.393	-2.120 ± 0.117	-0.403 ± 0.081	1.200 ± 0.053

Supplementary Table 2. RAMPFIT[36] results. Identification of TII start (*t*2) and end (*t*1). Uncertainties (σ1) gained using wild bootstrap (uncertainties exclude age model uncertainties).

SST increase preceding TII

There are alternative explanations for the initial SST increase observed in our study around ~135 ka. However, we explain below why those are not possible:

a) A shift in the ITCZ is not a contributor to the SST increase as if this were the case we would observe a synchronous change in both SST and ISM rainfall and runoff (the ITCZ has been interpreted as the sub-tropical manifestation of the ISM[98]). Our records instead show a decoupling of ~1 kyr between SST and ISM precipitation strength (Fig 2B n, o)

b) Similarly, a contributor of SST change associated with increased river discharge would also be seen in the $\delta^{18}O_{sw\text{-}IVC}$ which we do not observe (Fig 2B n, o).

c) Finally, we also find it unlikely that any contribution from upwelling changes contributed to the SST increase. If upwelling intensity were to increase at this interval then we would expect a decrease in SST associated with supply of colder upwelled waters in the surface layers. In contrast, if the upwelling intensity were to decrease then it would be manifested in the water column stratification through freshwater induced stratification[99]. Furthermore, we find no evidence of upwelling in an abundance record of a key upwelling indicator species of planktic foraminifera (*Globigerinoides bulloides*), a subpolar species that can be found in areas of upwelling in the tropics[100]. We observe no consistent relationship between SST and abundance of this species (Supplementary Figure 12).

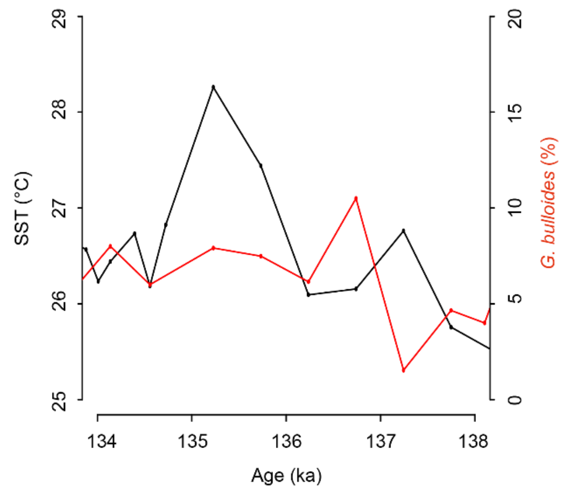

Supplementary Figure 12. Comparison of *G. bulloides* % (red) with SST (black).

Supplementary References

96. North Greenland Ice Core Project members. High-resolution record of Northern Hemisphere climate extending into the last interglacial period. *Nature*. **431,** 147-151 (2004).

97. Svensson, A. *et al*. A 60 000 year Greenland stratigraphic ice core chronology. *Clim. Past*. **4,** 47-47 (2008).

98. Chao, W. C. & Chen, B. The Origin of Monsoons. *J. Atmos. Sci.* **58,** 3497-3507 (2001).

99. Han, W., McCreary Jr., J. P. & Kohler, K. E. Influence of precipitation minus evaporation and Bay of Bengal rivers on dynamics, thermodynamics, and mixed layer physics in the upper Indian Ocean. *J. Geophys. Res.* **106,** 6895-6916 (2001).

100. Conan, S. M. –H. & Brummer, G. J. A. Fluxes of planktic foraminifera in response to monsoonal upwelling on the Somalia Basin margin. *Deep Sea Research Part II: Tropical Studies in Oceanography*. **47,** 2207-2227 (2000).